Contents lists available at ScienceDirect

Biosensors and Bioelectronics

Unleashing inkjet-printed nanostructured electrodes and battery-free potentiostat for the DNA-based multiplexed detection of SARS-CoV-2 genes

Marianna Rossetti [a,1,*], Chawin Srisomwat [b,1], Massimo Urban [a,c], Giulio Rosati [a,**], Gabriel Maroli [a,c,d], Hatice Gödze Yaman Akbay [a], Orawon Chailapakul [b], Arben Merkoçi [a,e,***]

[a] Catalan Institute of Nanoscience and Nanotechnology, UAB Campus, 08193, Bellaterra, Barcelona, Spain
[b] Electrochemistry and Optical Spectroscopy Center of Excellence (EOSCE), Department of Chemistry, Faculty of Science, Chulalongkorn University, Pathumwan, Bangkok, 10330, Thailand
[c] Universitat Autònoma de Barcelona, Campus de la UAB, Bellaterra, Barcelona, 08193, Spain
[d] Instituto de Investigaciones en Ingeniería Eléctrica Alfredo Desages (IIIE), Universidad Nacional del Sur, CONICET, Avenida Colón 80 Bahía Blanca, Buenos Aires, Argentina
[e] ICREA Institució Catalana de Recerca i Estudis Avançats, Passeig Lluís Companys 23, 08010, Barcelona, Spain

ARTICLE INFO

ABSTRACT

Following the global COVID-19 pandemic triggered by SARS-CoV-2, the need for rapid, specific and cost-effective point-of-care diagnostic solutions remains paramount. Even though COVID-19 is no longer a public health emergency, the disease still poses a global threat leading to deaths, and it continues to change with the risk of new variants emerging causing a new surge in cases and deaths. Here, we address the urgent need for rapid, cost-effective and point-of-care diagnostic solutions for SARS-CoV-2. We propose a multiplexed DNA-based sensing platform that utilizes inkjet-printed nanostructured gold electrodes and an inkjet-printed battery-free near-field communication (NFC) potentiostat for the simultaneous quantitative detection of two SARS-CoV-2 genes, the ORF1ab and the N gene. The detection strategy based on the formation of an RNA-DNA sandwich structure leads to a highly specific electrochemical output. The inkjet-printed nanostructured gold electrodes providing a large surface area enable efficient binding and increase the sensitivity. The inkjet-printed battery-free NFC potentiostat enables rapid measurements and real-time data analysis via a smartphone application, making the platform accessible and portable. With the advantages of speed (5 min), simplicity, sensitivity (low pM range, ~450% signal gain) and cost-effectiveness, the proposed platform is a promising alternative for point-of-care diagnostics and high-throughput analysis that complements the COVID-19 diagnostic toolkit.

1. Introduction

The COVID-19 pandemic caused by SARS-CoV-2 has spread rapidly across the globe since its emergence in late 2019, resulting in millions of confirmed cases and deaths (Msemburi et al., 2023; Schöley et al., 2023; Wang et al., 2022). Although COVID-19 is no longer a public health emergency (McCoy, 2023; Murray, 2022; Sarker et al., 2023; Wise, 2023), the disease still poses a global threat that causes deaths, and it continues to change with the risk of new variants emerging, leading to new increases in cases and deaths (Abulsoud et al., 2023; Karim and Karim, 2021; Wang et al., 2023). Diagnostic tests have played a crucial

role in detecting, containing and monitoring the COVID-19 pandemic (Lukas et al., 2020; Peeling et al., 2022; Udugama et al., 2020a). The tests enable early identification of infected individuals, allowing for immediate isolation and treatment, which can reduce transmission rates (Kucharski et al., 2020). In addition, the tests provide valuable data on the spread of the virus, allowing health authorities to track and respond to outbreaks (Hellewell et al., 2020).

Currently, COVID-19 detection methods are divided into molecular and serological tests (Udugama et al., 2020b). Molecular tests detect the viral RNA of SARS-CoV-2 in the early stages of infection and are highly sensitive and specific, but require long analysis times (4–5 h), expensive

instruments and reagents, and specialized personnel (Feng et al., 2020). Serological tests, on the other hand, detect SARS-CoV-2 antibodies (Wang et al., 2020) or proteins (Baumgarth et al., 2020) associated with the virus, including the spike protein (S), the nucleocapsid protein (N), and the receptor-binding domain (RBD) of the S protein. Serological tests are less sensitive and specific than molecular tests (Lisboa Bastos et al., 2020). In addition, SARS-CoV-2 antibodies (IgG and IgM), which are specific indicators of infection, usually peak several weeks after infection, making early detection of infection difficult (Post et al., 2020).

As early and rapid detection of infection is critical for effective treatment in the event of a pandemic, the development of point-of-care tests (POCTs) for the rapid, accurate, specific and cost-effective detection of SARS-CoV-2 is required (Weiss et al., 2020). POCTs are diagnostic tests that can be performed at or near the point of care and provide immediate results without the need for complex laboratory equipment or trained personnel. In recent years, considerable efforts have been made to develop rapid, inexpensive, easy-to-use, quantitative and sensitive point-of-care diagnostic devices for various diseases, including COVID-19 (Kabay et al., 2022; Kummari et al., 2023; Panicker et al., 2024; Rao Bommi et al., 2023; Rosati et al., 2021). Lateral flow immunoassays (LFAs) are one type of POCT that have gained popularity due to their ease of use, low cost and ability to work with untreated clinical samples (Rubio-Monterde et al., 2023). However, LFAs may not be as sensitive or specific as other diagnostic methods (Böger et al., 2021). In medical diagnostics, the personal blood glucose meter, which allows for regular self-monitoring of blood glucose levels, remains unsurpassed because it is quantitative, inexpensive, and easy to use (Lisi et al., 2020). Indeed, electrochemical sensors are ideal for POCTs because they can work effectively in complex sample matrices, require inexpensive instrumentation, can be easily mass-produced and have multiplexing capabilities (Ambaye et al., 2021; Fernandes et al., 2020).

Inkjet printing technologies have revolutionized electrode manufacturing, enabling faster, less expensive and more precise fabrication than traditional methods (Ambaye et al., 2021; Baek et al., 2022; Grillo et al., 2022; Jeong et al., 2022). Inkjet printing is a non-contact, digital printing process that uses specialized printers to deposit precise amounts of conductive inks onto various substrates (Donie et al., 2021; Tagliaferri et al., 2021). This technology offers several advantages, including the ability to create complex patterns with high resolution, the possibility to use a wide range of nanomaterial-based inks, and the flexibility to produce electrodes in large quantities with high reproducibility (Fukuda et al., 2013; Jarošová et al., 2019; Kim et al., 2023; Kokubo et al., 2019; Moya et al., 2017; Sundriyal and Bhattacharya, 2017). In addition, electrodes produced with inkjet printers can be easily integrated into smartphone-based sensing systems (Bai et al., 2021; Rosati et al., 2022). Recently, near-field communication (NFC) potentiostats, which are about the size of a credit card, have emerged as the simplest form of portable battery-free potentiostats (Beck et al., 2023; Krorakai et al., 2021; Steinberg et al., 2015). They take advantage of NFC's wireless communication, which enables short-range communication between electronic tags and smartphones (Kassal et al., 2013; Lazaro et al., 2022; Promsuwan et al., 2023; Pungjunun et al., 2022; Steinberg et al., 2015). NFC potentiostats, operating wirelessly *via* a smartphone with a user-friendly application for electrochemical analysis, provide a portable and affordable system with analytical capabilities comparable to those of conventional benchtop potentiostats (Beck et al., 2023).

Over the past decade, DNA nanotechnology has emerged as a rapidly growing field of research in which synthetic DNA strands are used to build structures and devices with remarkable precision at the nanoscale (Chou, 2021; Lacroix and Sleiman, 2021; Martynenko et al., 2021; Ricci and Dietz, 2023). This has led to the development of innovative sensing approaches for the detection of a wide range of targets (Hu et al., 2023; Ranallo et al., 2023; Rossetti and Porchetta, 2018; Zhang et al., 2023). However, to date, there are only a few examples of the detection of the viral nucleic acid SARS-CoV-2 by combining the advantages of

electrochemical sensors with those of DNA nanotechnology, most of which are based on sophisticated techniques (Fan et al., 2021; Hwang et al., 2021; Khan et al., 2020; Qiu et al., 2020; Santhanam et al., 2020; Sathish et al., 2021). A simple electrochemical platform using graphene and gold nanoparticles and employing antisense oligonucleotides was reported by Pan and coworkers (Alafeef et al., 2020). However, the proposed platform is limited to the detection of a single gene (*i.e.*, the viral N gene of SARS-CoV-2). According to WHO recommendations, molecular diagnostic tests for SARS-CoV-2 should target at least two different regions of the viral genome to minimize the risk of false negative results due to the high mutation rate of the virus ("Laboratory testing for 2019 novel coronavirus (2019-nCoV) in suspected human cases," n.d.). Indeed, simultaneous detection of multiple genes can improve the accuracy of SARS-CoV-2 diagnosis, especially in patients with low viral load (Chaibun et al., 2021; Kim et al., 2021; Tombuloglu et al., 2022).

Here, we propose a multiplexed *signal-on* DNA-based platform for the quantitative detection of ORF1ab and N genes by using a simple one-step sandwich hybridization detection strategy, gold nanoparticle-based nanostructured low-cost inkjet-printed electrodes, and a battery-free NFC potentiostat (Fig. 1). The detection strategy is based on the simultaneous targeting of the viral ORF1ab gene and the N gene by binding a pair of antisense oligonucleotides for each gene, a thiol-modified oligonucleotide acting as a capture probe and a redox-labeled oligonucleotide acting as a signal probe. The binding of the target to the two specific probes (*i.e.*, capture and signaling probes) results in a highly specific electrochemical output, due to the formation of an RNA-DNA sandwich. The enhanced nanostructuration of the gold electrodes, produced by combining inkjet printing with an alternative sintering protocol (Urban et al., 2023), increases the sensitivity of the electrochemical assay thanks to the large active surface area of the electrodes, which increases the number of capture sites and improves the accessibility of the target to the capture probe immobilized on the working electrode. An NFC module enables measurements and real-time data monitoring for better accessibility and portability.

2. Experimental section

Materials and specific experimental procedures, including reagents, oligonucleotides, production of inkjet-printed gold electrodes, preparation of the DNA-functionalized electrodes, electrochemical measurements, NFC-potentiostat design and production, are reported in the supporting information.

3. Results and discussion

3.1. Inkjet Printed Electrodes (IPEs) fabrication and characterization

We propose an electrochemical platform for the selective and sensitive detection of SARS-CoV-2 viral RNA using inkjet-printed nanostructured gold electrodes and antisense oligonucleotides as highly specific sensing elements. First, nanostructured inkjet-printed electrodes (IPEs) were fabricated by a method recently introduced by our group (Urban et al., 2023), which allows precise control of size and surface morphology (Fig. 2a–c, Fig. S1, S2). The active surface area of these printed electrodes calculated from the gold oxide reduction peak area of cyclic voltammograms under acidic conditions (*i.e.*, H_2SO_4 0.05 M) (Xiao et al., 2007) is 3.2 ± 0.2 cm^2, with a roughness factor (calculated as the ratio of real to geometric area) of 28 ± 2, which is more than 10 times higher than that of smooth electrodes (*i.e.*, screen-printed electrodes) (Fig. 2d and Table S1). The heterogeneous electron transfer constant k^0 extrapolated from cyclic voltammetry measurements in [Fe(CN)$_6$]$^{3-/4-}$ (2.5 mM in PBS 10 mM), at different scan rates, using the Nicholson method (Nicholson, 1965; Nicholson and Shain, 1964), shows that IPEs outperform classic smooth screen-printed electrodes by more than a factor of two, with a k^0 of 0.0261 cm s^{-1} and 0.098 cm s^{-1},
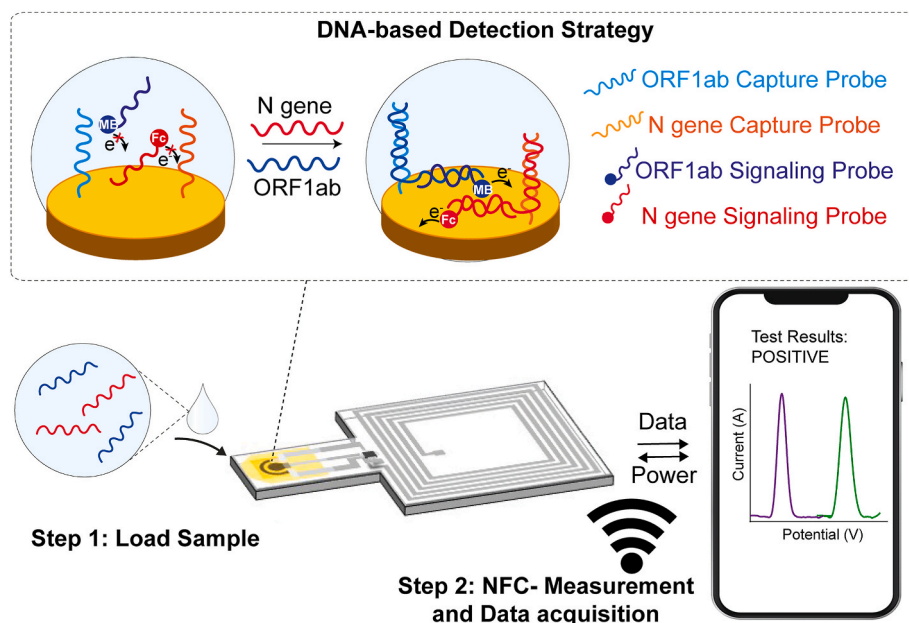
Fig. 1. Schematic representation of the working principle of the electrochemical sensing platform. In step 1, the viral RNA is dropped onto the electrode. In step 2, the NFC potentiostat allows to perform the electrochemical measurements *via* a smartphone. The digital electrochemical output is transmitted wirelessly *via* NFC. In the inset, the DNA-based detection strategy: ORF1ab and N gene capture probes are immobilized on the gold electrode. The ORF1ab and N gene labeling probes, which are labeled with methylene blue (MB) and ferrocene (Fc), respectively, are free in the solution. In the presence of the targets (ORF1ab and N gene), the formation of RNA-DNA duplexes brings the redox tags close to the electrode surface. This proximity enables electron transfer, which leads to the appearance of two different peaks.
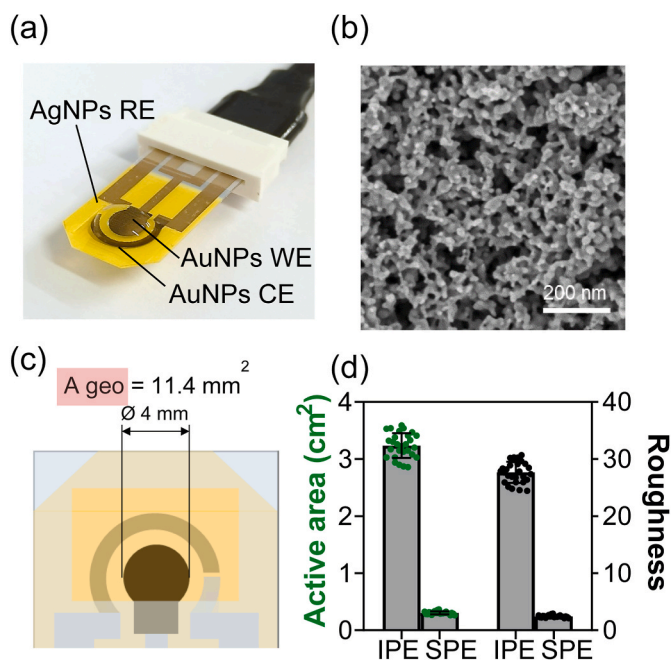

Fig. 2. Bare IPE Characterization. (**a**) Image of IPE. (**b**) SEM image of the IPE. (**c**) Design of the IPE. (**d**) Active area and roughness of the IPEs compared to commercial screen printed electrodes (SPEs) of comparable geometric area.

respectively, and a peak-to-peak distance of 77 *versus* 91 mV at a scan rate of 0.025 V s^{-1}. These results indicate that porosity and nanostructuration are an important factor in improving electroanalytical performance, even for low-cost disposable platforms (Fig. S3).

Since the extent of nanostructuring can affect the sensitivity of DNA-based sensors, (Bin et al., 2010) we evaluated the achievable surface coverage of DNA probes by ACV measurements (Rossetti et al., 2020) to determine the optimal density of capture probes. Our results show that our IPEs allow a surface coverage between $3.6 \pm 0.3 \times 10^{10}$ molecules/cm^2 and $5.5 \pm 0.5 \times 10^{10}$ molecules/cm^2. This corresponds to an average distance between capture probes ranging from 59 ± 2 nm to 47 ± 1 nm (Fig. 3a and Table S2). Next, we performed square-wave voltammetry measurements in the presence of methylene blue (MB) and ferrocene (Fc), first individually and then simultaneously, to determine the electrochemical response of our IPEs and the suitability of MB and Fc as tags for the signaling ss-DNA probes (Kang et al., 2016). As expected, our results clearly demonstrate the feasibility of using these two redox tags to label the two signaling probes without causing interference (Fig. 3b). In addition, we also investigated the response of the bare electrodes as a function of increasing redox tags concentration (Fig. S4). We observed a different electrochemical response of the two redox tags, which can be attributed to their different hydrophobicity affecting the electronic transfer (Cunnane et al., 1995; Poli et al., 2020; Su et al., 2021) as well as the peculiar electron transfer tacking place in nanoporous electrodes (Daggumati et al., 2015; Matharu et al., 2017; Park et al., 2012).
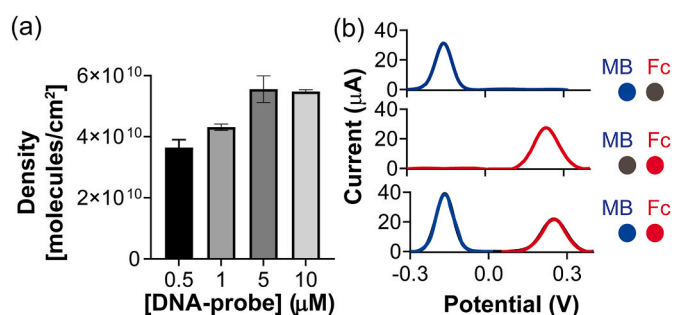
Fig. 3. (**a**) Surface coverage of DNA probe. (**b**) Raw SWV profiles from top to bottom of a solution of 50 μM MB, a solution of 1.25 mM Fc, and a solution of both redox tags (*i.e.*, 50 μM MB +1.25 mM Fc), clearly showing that it is possible to detect MB and Fc simultaneously without any interference.

3.2. Detection strategy

Based on the previous results, a "signal-on" sandwich hybridization assay was designed for the specific detection of the ORF1ab gene and the N gene. Thiol-modified antisense oligonucleotides (*i.e.*, ssDNA-capture probes) and redox-labeled antisense oligonucleotides (*i.e.*, ssDNA-signaling probes) were designed for each gene. The capture probes and signaling probes both consist of 15 bases and bind to two adjacent gene regions. A 15 bp length guarantees a strong and specific duplex formation between DNA and RNA. In fact, a minimum of 6–8 contiguous base pairs is required for stable duplex formation (Banerjee et al., 2021, 2023; Breslauer et al., 1986; Cisse et al., 2012; Ghosh et al., 2020; Ma et al., 2004; Owczarzy et al., 1997; Sugimoto et al., 1994, 1995). Therefore, the 15 base pairs in our DNA probes significantly exceeding this minimum threshold, provide a reliable and specific binding mechanism. In the presence of the specific RNA target, an RNA-DNA sandwich consisting of the ss-DNA capture probe, the target RNA and ssDNA-signaling probe is formed and generates an electrochemical output due to the electron transfer between the redox tag and the nanoporous gold surface. The ssDNA-capture probes were immobilized onto the gold working electrode *via* sulfur-gold chemistry. To distinguish the response with respect to the two genes, we tagged the two ssDNA-signaling probes with two different redox tags at one end (*i.e.*, MB and Fc for the ORF1ab and N genes, respectively) (Fig. 1). We note that the ssDNA-signaling probes were designed to hybridize with the downstream positions of the target RNAs, ensuring efficient electron transfer between the redox tag and the gold electrode surface (Idili et al., 2014; Jampasa et al., 2018; Rowe et al., 2011).

First, we performed electrochemical impedance spectroscopy (EIS) measurements to characterize each step of sensor fabrication (Fig. S5 and Table S3). In this experiment, we first measured the R_{CT} of the bare electrode (step 1), then we immobilized the DNA capture probe (step 2). The immobilization of the DNA capture probe leads to an increase in the R_{CT} value from 56 ± 2 Ω to 840 ± 10 Ω. This change is due to the enhanced repulsive interactions (electrostatic and steric) between the redox maker ions (i.e., $[Fe(CN)_6]^{3-/4-}$) and the electrode surface modified with the DNA capture probe; the repulsion hinders the charge transfer through the interface (Ito et al., 2007; Karimizefreh et al., 2017). In the following step (step 3), we passivated the electrode surface with MCH and we found a much larger R_{CT} value (1760 ± 10 Ω). This behavior is due to the fact that MCH prevents charge transfer between electrolyte and electrode surface due to electrostatic and steric repulsion (Butterworth et al., 2019; Karimizefreh et al., 2017). In the following step 4, we added the RNA target and obtained a decrease in the R_{CT} value due to the formation of the partial complementary duplex ($R_{CT} = 649 \pm 5$ Ω). Although this electrochemical behavior seems counterintuitive because the duplex formation would increase the negative charge at the electrode surface and the electrostatic repulsion of the redox marker ions would increase the R_{CT} value, this has been previously reported by other authors (Gooding et al., 2003; Ito et al., 2007; Pan and Rothberg, 2005; Piro et al., 2005; Wei et al., 2003). We speculate that steric repulsion of surface-bound DNA may be the predominant barrier to access of marker ions to the surface in our sensor system. It is known that this effect is reduced by the formation of a duplex (Gooding et al., 2003; Piro et al., 2005). In the last step (step 5), we added the signalling probe to achieve full duplex formation. In this case, we observed an increase in R_{CT} (2080 ± 20 Ω), which could be due to a structural distortion of the surface-bound duplex and to the increase in electrostatic repulsion of the redox marker ions with the longer duplex formation, which would double the negative charge at the electrode surface (Bardea et al., 1999; Patolsky et al., 2001).

Second, we characterized the analytical performance of the sensor (Fig. 4a and b, Fig. S6, S7, Tables S4 and S5) by collecting the electrochemical signal in the presence of increasing concentrations of target (*i. e.*, synthetic fragments of ORF1ab and N genes). As expected, the presence of the target induces the formation of the sandwich complex, which increases the current signal (up to $420\% \pm 9\%$ for the ORF1ab gene and up to $454\% \pm 4\%$ for the N gene). By fitting the data with a four-parameter logistic equation, we estimated an inflection point ($K_{1/2}$) of 19.0 ± 0.5 nM for the ORF1ab gene and of 18.8 ± 0.9 nM for N gene. The dynamic range, calculated as the concentration range that induces a signal change between 10% and 90% of the maximum signal gain, is from 1.3 nM to 294 nM for ORF1ab and from 0.9 nM to 159 nM for Ngene (Fig. S6). The limits of detection (LODs) were calculated based on the standard deviation of the response (Sy) of the curve and the slope of the binding curve (S) at values approximating the LOD according to the formula: LOD = 3.3(Sy/S), are estimated to be 93 pM for ORF1ab and 96 pM for Ngene (Fig. S7). The hybridization rate is fast and reaches the plateau of the current in about 5 min in the presence of a saturating concentration of the target (*i.e.*, 3 µM) ($t_{1/2} = 0.45 \pm 0.05$ min for ORF1ab and 0.52 ± 0.07 min for Ngene) (Fig. 4c). As a control experiment, we performed binding curves by adding only the ORF1ab gene in the absence of the N gene and *vice versa*. We obtained no cross-reactivity responses and no significant difference in signal gain when we tested the gene individually or simultaneously with the other gene. Indeed, the peak of ferrocene associated with the presence of the N gene remained constant when we added only the ORF1ab gene, and analogously, the peak of MB associated with the presence of the ORF1ab gene remained constant when we added only the N gene (Fig. S8). We also conducted a further experiment to confirm that the exclusive mechanism for MB reduction occurs directly at the electrode surface and that there is no discernible contribution from the intercalation of MB within the duplex (Kang et al., 2009, 2016; Pheeney and Barton, 2012) (Fig. S9).

We then tested the sensor with longer synthetic SARS-CoV-2 RNA fragments (see Materials and Methods in Supplementary Information) consisting of six non-overlapping 5 kb fragments covering 99.9% of the viral genome and containing ORF1ab and N genes split over several fragments. Binding curves obtained by adding increasing concentration of viral control show a $K_{1/2}$ of 200 ± 30 copies/µL for ORF1ab gene, and of 210 ± 20 copies/µL for N gene (Fig. 5a and b) with a dynamic range from 30 copies/µL to 1180 copies/µL for ORF1ab and from 17 to 2600 copies/µL for N gene (Fig. S10).

3.3. Development of the DNA-based platform combining IPEs and battery-free NFC Potentiostat

After demonstrating the ability of our sensor to simultaneously detect SARS-CoV-2 RNA targets, we developed an inkjet-printed single-chip flexible biosensor, incorporating an antenna optimized for NFC energy harvesting, which allows to perform and collect the data *via* an Android application (Fig. 6a and b and Fig. S11). NFC is a protocol for wireless data exchange within a very short range, usually limited to about 5 cm. NFC operates at a frequency of 13.56 MHz, as defined in the ISO/IEC 18000-3 standard, and enables data transmission speeds varying of 106 kbit/s to 424 kbit/s. The technology uses loop antennas, which are characterized by an inductance that must be precisely matched to the internal capacitance of the intended chip to ensure that the resonant frequency between the antenna and the chip's internal capacitor is tuned to the required 13.56 MHz. To bring the inductance to the required level, it is possible to integrate external capacitors to reduce the required inductance value. The parasitic capacitance created by the inductor itself must also be considered when designing these systems (Maroli et al., 2021). By employing a NFC-enabled SIC4341 potentiostat, operating according to the ISO14443A standard, we engineered a low-cost integrated circuit (with an estimated approximate price of 1.50) (Maroli et al., 2023). This NFC device allows electrochemical measurements to be performed and the current and voltage to be properly adjusted from ± 20 µA and ± 0.8 V, respectively, through the use of an app (*i.e.*, Chemister APP by Silicon Craft Technology). In particular, we utilized the capability of NFC at 13.56 MHz to enable both energy harvesting and data transmission simultaneously. Unlike other works that use the same integrated potentiostat and where the
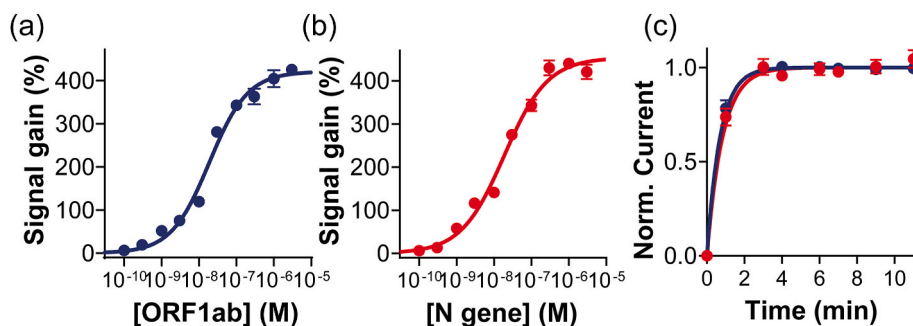
Fig. 4. Quantitative simultaneous detection of synthetic fragments of (**a**) ORF1ab gene and (**b**) N gene. (**c**) Kinetic of hybridization when the sensor is tested with a saturating concentration (*i.e.*, 3 μM) of target (*i.e.*, ORF1ab in blue, N gene in red).
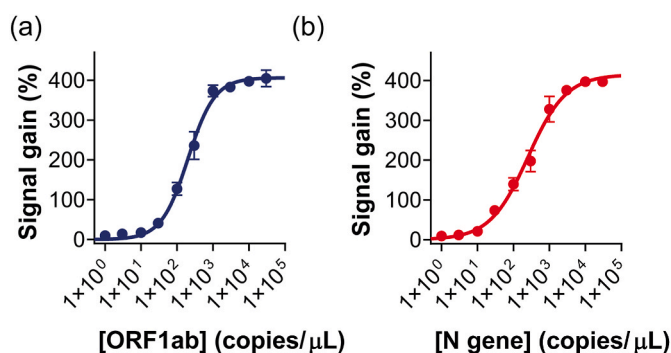

Fig. 5. Quantitative simultaneous detection of (**a**) ORF1ab gene and (**b**) N gene, obtained by adding increased concentration of six 5 kb non-overlapping synthetic viral RNA fragments covering 99.9% of the viral genome.

manufacturer's demo board is used primarily as a proof of concept, here we developed an antenna that was printed and fully integrated into the final device. The antenna was carefully fabricated, keeping the trace width (w), spacing (s), and turn count (n) constant (1.5 mm, 0.25 mm and 5, respectively), while the outer diameter (D_{out}) was tuned to a final size of 54 mm. The resulting inductor length of 897.8 mm yielded an electrical resistance very close to the empirical measurement of 36.6 Ω (Figs. S12 and S13), giving an inductance (L) of 2.13 μH and a quality factor (Q) of 5.67.

To test our battery-free NFC potentiostat, we first added increased concentrations of redox tags (*i.e.*, MB and Fc) (Fig. 6c) and obtained results comparable to those obtained by using a benchtop potentiostat (Figs. S4 and S14). Following these results, we tested the platform for the detection of ORF1ab and N gene, under the same conditions as before. Also in this case, our results showed that our platform is capable of the simultaneous detection of both genes (Fig. 6d).

4. Conclusions

Here we have designed and developed a highly versatile and cost-effective DNA-based sensor platform to detect RNA fragments in rapid time and without washing steps. We have developed capture and signaling probes that respond simultaneously to two different genes without interfering with each other. We have printed nanostructured electrodes with increased surface area that provide a larger number of sites for the capture probes and also improve accessibility during hybridization, resulting in fast and efficient binding. We integrated our inkjet-printed electrodes with an NFC potentiostat that allows measurements to be performed and data to be collected in real time using a smartphone. The direct printing of the antenna together with the electrode increases the cost-effectiveness of the device with a production cost of about €2 (Table S6) and a production time in the order of minutes. We would like to emphasize that the total cost of the single device

can be significantly reduced by bulk purchases. This economic perspective not only improves the practicality of our device, but also opens up opportunities for scalable production, enhancing the potential impact of our work in real-world applications. It is worth noting that our multiplexing single-step direct sensing method does not rely on an amplification step and therefore does not achieve the sensitivity of the gold standard real-time reverse transcription polymerase chain reaction (RT-PCR) (Kubina and Dziedzic, 2020). However, our platform is promising as it enables a fast response (5 min) without multi-step, wash- and reagent-intensive processes. In addition, the cost of our platform is much lower than the cost of RT-PCR, because unlike RT-PCR, which is not only reagent-intensive but also requires well-trained technicians, our platform does not require specialized technicians and the measurements are performed with a low-cost, portable potentiostat using a standard smartphone. Further validation is required, especially for high viral load samples, such as saliva, which could potentially be detected without an amplification step (Herrera et al., 2021). In our upcoming studies, we aim to validate the effectiveness of our sensing platform by testing it with real samples. The specificity of the sensor, which targets 30 bases within the SARS-CoV-2 genes, makes us confident that we will be able to detect ORF1ab and the N gene in real samples. We believe that the proposed platform, which enables rapid, accessible and cost-effective detection of SARS-CoV-2, is a valuable addition to the COVID-19 diagnostic toolkit. Although different detection kits are available on the market, our platform is characterized by the simultaneous detection of two different genes, which enables a higher accuracy in COVID diagnosis. Finally, we would like to emphasize that this platform can be easily adapted for the detection of other viruses as well as long non-coding RNAs by simply changing the sequences of the capture and signaling probes. This requires designing probes with bases that are complementary to specific regions of the target virus, thus expanding the platform's applications. In summary, our multiplexed, single-step, signal-ON platform is a promising solution for point-of-care diagnostics and high-throughput analysis.

CRediT authorship contribution statement

Marianna Rossetti: Writing – original draft, Visualization, Supervision, Methodology, Investigation, Formal analysis, Data curation. **Chawin Srisomwat:** Writing – original draft, Visualization, Investigation, Conceptualization. **Massimo Urban:** Writing – original draft, Methodology, Investigation. **Giulio Rosati:** Supervision, Formal analysis, Data curation, Conceptualization. **Gabriel Maroli:** Writing – original draft, Methodology, Investigation. **Hatice Gödze Yaman Akbay:** Investigation. **Orawon Chailapakul:** Resources. **Arben Merkoçi:** Supervision, Resources, Project administration, Funding acquisition.

Declaration of competing interest

The authors declare that they have no known competing financial
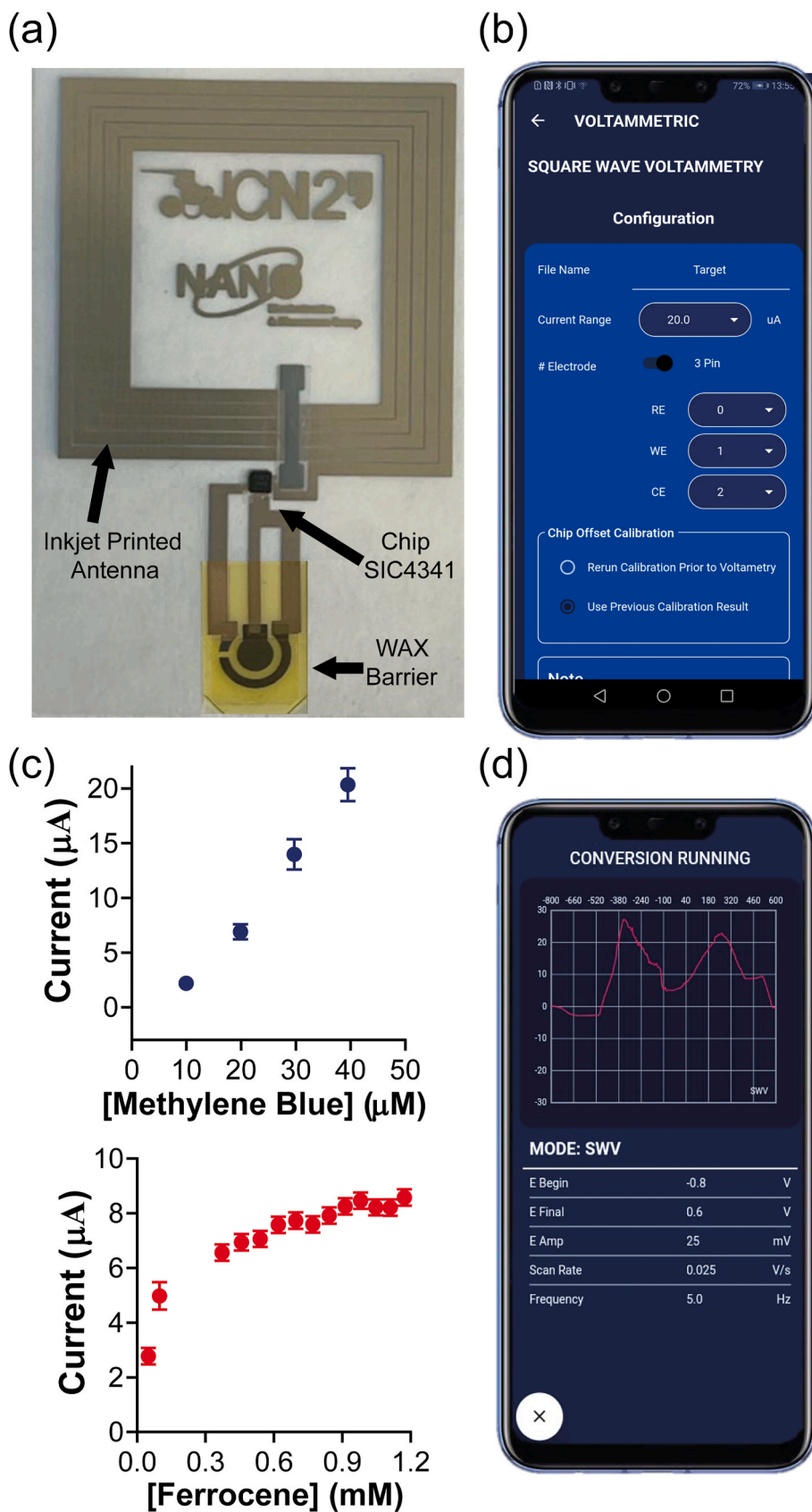
Fig. 6. (a) Picture of inkjet printed antenna with IPE electrode. (**b**) App interface picture. (**c**) Calibration curves of MB and Fc obtained by adding increasing concentration of redox tag on the IPE using the NFC battery-free potentiostat. (**d**) Square wave voltammetry profile obtained when the platform is tested with saturating concentrations of target (*i.e.*, ORF1 ab and N gene, 3 μM).

interests or personal relationships that could have appeared to influence the work reported in this paper.

Data availability

Data will be made available on request.

Acknowledgements

Appendix A. Supplementary data

Supplementary data to this article can be found online at https://doi.org/10.1016/j.bios.2024.116079.

References

Abulsoud, A.I., El-Husseiny, H.M., El-Husseiny, A.A., El-Mahdy, H.A., Ismail, A., Elkhawaga, S.Y., Khidr, E.G., Fathi, D., Mady, E.A., Najda, A., Abdel-Daim, M.M., Doghish, A.S., 2023. Mutations in SARS-CoV-2: insights on structure, variants, vaccines, and biomedical interventions. Biomed. Pharmacother. 157 https://doi.org/10.1016/j.biopha.2022.113977.

Alafeef, M., Dighe, K., Moitra, P., Pan, D., 2020. Rapid, ultrasensitive, and quantitative detection of SARS-CoV-2 using antisense oligonucleotides directed electrochemical biosensor chip. ACS Nano 14, 17028–17045. https://doi.org/10.1021/ACSNANO.0C06392/ASSET/IMAGES/LARGE/NN0C06392_0010 (JPEG).

Ambaye, A.D., Kefeni, K.K., Mishra, S.B., Nxumalo, E.N., Ntsendwana, B., 2021. Recent developments in nanotechnology-based printing electrode systems for electrochemical sensors. Talanta 225. https://doi.org/10.1016/j.talanta.2020.121951.

Baek, S., Lee, Y., Baek, J., Kwon, J., Kim, S., Lee, S., Strunk, K.-P., Stehlin, S., Melzer, C., Park, S.-M., Ko, H., Jung, S., 2022. Spatiotemporal measurement of arterial pulse waves enabled by wearable active-matrix pressure sensor arrays. ACS Nano 16, 368–377. https://doi.org/10.1021/acsnano.1c06695.

Bai, Y., Guo, Q., Xiao, J., Zheng, M., Zhang, D., Yang, J., 2021. An inkjet-printed smartphone-supported electrochemical biosensor system for reagentless point-of-care analyte detection. Sensor. Actuator. B Chem. 346 https://doi.org/10.1016/j.snb.2021.130447.

Banerjee, D., Tateishi-Karimata, H., Ohyama, T., Ghosh, S., Endoh, T., Takahashi, S., Sugimoto, N., 2021. Improved nearest-neighbor parameters for the stability of RNA/DNA hybrids under a physiological condition. Nucleic Acids Res. 48, 12042–12054. https://doi.org/10.1093/nar/gkaa572.

Banerjee, D., Tateishi-Karimata, H., Toplishek, M., Ohyama, T., Ghosh, S., Takahashi, S., Trajkovski, M., Plavec, J., Sugimoto, N., 2023. In-cell stability prediction of RNA/DNA hybrid duplexes for designing oligonucleotides aimed at therapeutics. J. Am. Chem. Soc. 145, 23503–23518. https://doi.org/10.1021/jacs.3c06706.

Baumgarth, N., Nikolich-Žugich, J., Lee, F.E.-H., Bhattacharya, D., 2020. Antibody responses to SARS-CoV-2: let's stick to known knowns. J. Immunol. 205, 2342–2350. https://doi.org/10.4049/JIMMUNOL.2000839.

Beck, J.J., Alenicheva, V., Rahn, K.L., Russo, M.J., Baldo, T.A., Henry, C.S., 2023. Evaluating the performance of an inexpensive, commercially available, NFC-powered and smartphone controlled potentiostat for electrochemical sensing. Electroanalysis 35. https://doi.org/10.1002/elan.202200552.

Bin, X., Sargent, E.H., Kelley, S.O., 2010. Nanostructuring of sensors determines the efficiency of biomolecular capture. Anal. Chem. 82, 5928–5931. https://doi.org/10.1021/ac101164n.

Böger, B., Fachi, M.M., Vilhena, R.O., Cobre, A.F., Tonin, F.S., Pontarolo, R., 2021. Systematic review with meta-analysis of the accuracy of diagnostic tests for COVID-19. Am. J. Infect. Control 49, 21–29. https://doi.org/10.1016/J.AJIC.2020.07.011.

Breslauer, K.J., Frank, R., Blocker, H., Marky, L.A., 1986. Predicting DNA duplex stability from the base sequence. Proc. Natl. Acad. Sci. U.S.A. 83, 3746–3750. https://doi.org/10.1073/pnas.83.11.3746.

Butterworth, A., Blues, E., Williamson, P., Cardona, M., Gray, L., Corrigan, D.K., 2019. SAM composition and electrode roughness affect performance of a DNA biosensor for antibiotic resistance. Biosensors 9. https://doi.org/10.3390/BIOS9010022.

Chaibun, T., Puenpa, J., Ngamdee, T., Boonapatcharoen, N., Athamanolap, P., O'Mullane, A.P., Vongpunsawad, S., Poovorawan, Y., Lee, S.Y., Lertanantawong, B., 2021. Rapid electrochemical detection of coronavirus SARS-CoV-2. Nat. Commun. 12 https://doi.org/10.1038/s41467-021-21121-7.

Chou, L.Y.T., 2021. Design verification as foundation for advancing DNA nanotechnology applications. ACS Nano 15, 9222–9228. https://doi.org/10.1021/acsnano.1c04304.

Cisse, I.I., Kim, H., Ha, T., 2012. A rule of seven in Watson-Crick base-pairing of mismatched sequences. Nat. Struct. Mol. Biol. 19, 623–627. https://doi.org/10.1038/nsmb.2294.

Cunnane, V.J., Geblewicz, G., Schiffrin, D.J., 1995. Electron and ion transfer potentials of ferrocene and derivatives at a liquid-liquid interface. Electrochim. Acta 40, 3005–3014. https://doi.org/10.1016/0013-4686(95)00255-7.

Daggumati, P., Matharu, Z., Seker, E., 2015. Effect of nanoporous gold thin film morphology on electrochemical DNA sensing. Anal. Chem. 87, 8149–8156. https://doi.org/10.1021/acs.analchem.5b00846.

Donie, Y.J., Schlisske, S., Siddique, R.H., Mertens, A., Narasimhan, V., Schackmar, F., Pietsch, M., Hossain, I.M., Hernandez-Sosa, G., Lemmer, U., Lemmer, U., Gomard, G., 2021. Phase-separated nanophotonic structures by inkjet printing. ACS Nano 15, 7305–7317. https://doi.org/10.1021/acsnano.1c00552.

Fan, Z., Yao, B., Ding, Y., Zhao, J., Xie, M., Zhang, K., 2021. Entropy-driven amplified electrochemiluminescence biosensor for RdRp gene of SARS-CoV-2 detection with self-assembled DNA tetrahedron scaffolds. Biosens. Bioelectron. 178 https://doi.org/10.1016/j.bios.2021.113015.

Feng, W., Newbigging, A.M., Le, C., Pang, B., Peng, H., Cao, Y., Wu, J., Abbas, G., Song, J., Wang, D.B., Cui, M., Tao, J., Tyrrell, D.L., Zhang, X.E., Zhang, H., Le, X.C., 2020. Molecular diagnosis of COVID-19: challenges and research needs. Anal. Chem. 92, 10196–10209. https://doi.org/10.1021/ACS.ANALCHEM.0C02060/ASSET/IMAGES/LARGE/AC0C02060_0004. JPEG.

Fernandes, I.J., Aroche, A.F., Schuck, A., Lamberty, P., Peter, C.R., Hasenkamp, W., Rocha, T.L.A.C., 2020. Silver nanoparticle conductive inks: synthesis, characterization, and fabrication of inkjet-printed flexible electrodes. Sci. Rep. 10 https://doi.org/10.1038/s41598-020-65698-3.

Fukuda, K., Sekine, T., Kumaki, D., Tokito, S., 2013. Profile control of inkjet printed silver electrodes and their application to organic transistors. ACS Appl. Mater. Interfaces 5, 3916–3920. https://doi.org/10.1021/am400632s.

Ghosh, S., Takahashi, S., Ohyama, T., Endoh, T., Tateishi-Karimata, H., Sugimoto, N., Sugimoto, N., 2020. Nearest-neighbor parameters for predicting DNA duplex stability in diverse molecular crowding conditions. Proc. Natl. Acad. Sci. U.S.A. 117, 14194–14201. https://doi.org/10.1073/pnas.1920886117.

Gooding, J.J., Kanatzidis, M.G., Mearns, F.J., Wong, E., Leh, S., Jericho, K.L., 2003. The ion gating effect: using a change in flexibility to allow label free electrochemical detection of DNA hybridisation. Chem. Commun. 3, 1938–1939. https://doi.org/10.1039/b305798b.

Grillo, A., Peng, Z., Pelella, A., Di Bartolomeo, A., Casiraghi, C., 2022. Etch and print: graphene-based diodes for silicon technology. ACS Nano. https://doi.org/10.1021/acsnano.2c10684.

Hellewell, J., Abbott, S., Gimma, A., Bosse, N.I., Jarvis, C.I., Russell, T.W., Munday, J.D., Kucharski, A.J., Edmunds, W.J., Sun, F., Funk, S., Eggo, R.M., 2020. Feasibility of controlling COVID-19 outbreaks by isolation of cases and contacts. Lancet Global Health 8, e488–e496. https://doi.org/10.1016/S2214-109X(20)30074-7.

Herrera, L.A., Hidalgo-Miranda, A., Reynoso-Noverón, N., Meneses-García, A.A., Mendoza-Vargas, A., Reyes-Grajeda, J.P., Vadillo-Ortega, F., Cedro-Tanda, A., Peñaloza, F., Frías-Jimenez, E., Arriaga-Canon, C., Ruiz, R., Angulo, O., López-Villaseñor, I., Amador-Bedolla, C., Vilar-Compte, D., Cornejo, P., Cisneros-Villanueva, M., Hurtado-Cordova, E., Cendejas-Orozco, M., Hernández-Morales, J.S., Moreno, B., Hernández-Cruz, I.A., Herrera, C.A., García, F., González-Woge, M.A., Munguía-Garza, P., Luna-Maldonado, F., Sánchez-Vizcarra, A., Osnaya, V.G., Medina-Molotla, N., Alfaro-Mora, Y., Cáceres-Gutiérrez, R.E., Tolentino-García, L., Rosas-Escobar, P., Román-González, S.A., Escobar-Arrazola, M.A., Canseco-Méndez, J.C., Ortiz-Soriano, D.R., Domínguez-Ortiz, J., González-Barrera, A.D., Aparicio-Bautista, D.I., Cruz-Rangel, A., Alarcón-Zendejas, A.P., Contreras-Espinosa, L., González, R., Guerra-Calderas, L., Meraz-Rodríguez, M.A., Montalvo-Casimiro, M., Montiel-Manríquez, R., Torres-Arciga, K., Venegas, D., Juárez-González, V., Guajardo-Barreto, X., Monroy-Martínez, V., Guillén, D., Fernández, J., Herrera, J., León-Rodriguez, R., Canela-Pérez, I., Ruíz-Ordaz, B.H., Valdez-Vazquez, R., Bertin-Montoya, J., Niembro-Ortega, M., Villegas-Acosta, L., López-Castillo, D., Soriano-Ríos, A., Gastelum-Ramos, M., Zamora-Barandas, T., Morales-Baez, J., García-Rodríguez, M., García-Martínez, M., Nieto-Patlán, E., Quirasco-Baruch, M., López-Martínez, I., Ramírez-Gonzalez, E., Olivera-Díaz, H., Escobar-Escamilla, N., 2021. Saliva is a reliable and accessible source for the detection of

SARS-CoV-2. Int. J. Infect. Dis. 105, 83–90. https://doi.org/10.1016/J.IJID.2021.02.009.

Hu, Y., Duan, Y., Salaita, K., 2023. DNA nanotechnology for investigating mechanical signaling in the immune system. Angew. Chem. Int. Ed. 62 https://doi.org/10.1002/anie.202302967.

Hwang, C., Park, N., Kim, E.S., Kim, M., Kim, S.D., Park, S., Kim, N.Y., Kim, J.H., 2021. Ultra-fast and recyclable DNA biosensor for point-of-care detection of SARS-CoV-2 (COVID-19). Biosens. Bioelectron. 185, 113177 https://doi.org/10.1016/J.BIOS.2021.113177.

Idili, A., Amodio, A., Vidonis, M., Feinberg-Somerson, J., Castronovo, M., Ricci, F., 2014. Folding-upon-binding and signal-on electrochemical DNA sensor with high affinity and specificity. Anal. Chem. 86, 9013–9019. https://doi.org/10.1021/ac501418g.

Ito, T., Hosokawa, K., Maeda, M., 2007. Detection of single-base mismatch at distal end of DNA duplex by electrochemical impedance spectroscopy. Biosens. Bioelectron. 22, 1816–1819. https://doi.org/10.1016/J.BIOS.2006.08.008.

Jampasa, S., Siangproh, W., Laocharoensuk, R., Yanatatsaneejit, P., Vilaivan, T., Chailapakul, O., 2018. A new DNA sensor design for the simultaneous detection of HPV type 16 and 18 DNA. Sensor. Actuator. B Chem. 265, 514–521. https://doi.org/10.1016/J.SNB.2018.03.045.

Jarošová, R., McClure, S.E., Gajda, M., Jović, M., Girault, H.H., Lesch, A., Maiden, M., Waters, C., Swain, G.M., 2019. Inkjet-printed carbon nanotube electrodes for measuring pyocyanin and uric acid in a wound fluid simulant and culture media. Anal. Chem. 91, 8835–8844. https://doi.org/10.1021/acs.analchem.8b05591.

Jeong, I., Cho, K., Yun, S., Shin, J., Kim, J., Kim, G.T., Lee, T., Chung, S., 2022. Tailoring the electrical characteristics of MoS$_2$FETs through controllable surface charge transfer doping using selective inkjet printing. ACS Nano 16, 6215–6223. https://doi.org/10.1021/acsnano.2c00021.

Kabay, G., DeCastro, J., Altay, A., Smith, K., Lu, H.-W., Capossela, A.M., Moarefian, M., Aran, K., Dincer, C., 2022. Emerging biosensing technologies for the diagnostics of viral infectious diseases. Adv. Mater. 34 https://doi.org/10.1002/adma.202201085.

Kang, D., Ricci, F., White, R.J., Plaxco, K.W., 2016. Survey of redox-active moieties for application in multiplexed electrochemical biosensors. Anal. Chem. 88, 10452–10458. https://doi.org/10.1021/ACS.ANALCHEM.6B02376/SUPPL_FILE/AC6B02376_SI_001.PDF.

Kang, D., Zuo, X., Yang, R., Xia, F., Plaxco, K.W., White, R.J., 2009. Comparing the properties of electrochemical-based DNA sensors employing different redox tags. Anal. Chem. 81, 9109–9113. https://doi.org/10.1021/ac901811n.

Karim, S.S.A., Karim, Q.A., 2021. Omicron SARS-CoV-2 variant: a new chapter in the COVID-19 pandemic. Lancet 398, 2126–2128. https://doi.org/10.1016/S0140-6736(21)02758-6.

Karimizefreh, A., Mahyari, F.A., VaezJalali, M., Mohammadpour, R., Sasanpour, P., 2017. Impedimetic biosensor for the DNA of the human papilloma virus based on the use of gold nanosheets. Microchim. Acta 184, 1729–1737. https://doi.org/10.1007/s00604-017-2173-8.

Kassal, P., Steinberg, I.M., Steinberg, M.D., 2013. Wireless smart tag with potentiometric input for ultra low-power chemical sensing. Sensor. Actuator. B Chem. 184, 254–259. https://doi.org/10.1016/j.snb.2013.04.049.

Khan, M.Z.H., Hasan, M.R., Hossain, S.I., Ahommed, M.S., Daizy, M., 2020. Ultrasensitive detection of pathogenic viruses with electrochemical biosensor: state of the art. Biosens. Bioelectron. 166 https://doi.org/10.1016/j.bios.2020.112431.

Kim, D., Hong, N., Hong, W., Lee, J., Bissannagari, M., Cho, Y., Kwon, H.-J., Jang, J.E., Kang, H., 2023. Inkjet-printed polyelectrolyte seed layer-based, customizable, transparent, ultrathin gold electrodes and facile implementation of photothermal effect. ACS Appl. Mater. Interfaces 15, 20508–20519. https://doi.org/10.1021/acsami.3c01160.

Kim, H.E., Schuck, A., Lee, S.H., Lee, Y., Kang, M., Kim, Y.S., 2021. Sensitive electrochemical biosensor combined with isothermal amplification for point-of-care COVID-19 tests. Biosens. Bioelectron. 182 https://doi.org/10.1016/J.BIOS.2021.113168.

Kokubo, N., Arake, M., Yamagishi, K., Morimoto, Y., Takeoka, S., Ohta, H., Fujie, T., 2019. Inkjet-printed neural electrodes with mechanically gradient structure. ACS Appl. Bio Mater. 2, 20–26. https://doi.org/10.1021/acsabm.8b00574.

Krorakai, K., Klangphukhiew, S., Kulchat, S., Patramanon, R., 2021. Smartphone-based nfc potentiostat for wireless electrochemical sensing. Appl. Sci. 11, 1–13. https://doi.org/10.3390/app11010392.

Kubina, R., Dziedzic, A., 2020. Molecular and serological tests for COVID-19. A comparative review of SARS-CoV-2 coronavirus laboratory and point-of-care diagnostics. Diagnostics 10. https://doi.org/10.3390/diagnostics10060434.

Kucharski, A.J., Klepac, P., Conlan, A.J.K., Kissler, S.M., Tang, M.L., Fry, H., Gog, J.R., Edmunds, W.J., Emery, J.C., Medley, G., Munday, J.D., Russell, T.W., Leclerc, Q.J., Diamond, C., Procter, S.R., Gimma, A., Sun, F.Y., Gibbs, H.P., Rosello, A., van Zandvoort, K., Hué, S., Meakin, S.R., Deol, A.K., Knight, G., Jombart, T., Foss, A.M., Bosse, N.I., Atkins, K.E., Quilty, B.J., Lowe, R., Prem, K., Flasche, S., Pearson, C.A.B., Houben, R.M.G.J., Nightingale, E.S., Endo, A., Tully, D.C., Liu, Y., Villabona-Arenas, J., O'Reilly, K., Funk, S., Eggo, R.M., Jit, M., Rees, E.M., Hellewell, J., Clifford, S., Jarvis, C.I., Abbott, S., Auzenbergs, M., Davies, N.G., Simons, D., 2020. Effectiveness of isolation, testing, contact tracing, and physical distancing on reducing transmission of SARS-CoV-2 in different settings: a mathematical modelling study. Lancet Infect. Dis. 20, 1151–1160. https://doi.org/10.1016/S1473-3099(20)30457-6.

Kummari, S., Panicker, L.R., Rao Bommi, J., Karingula, S., Sunil Kumar, V., Mahato, K., Goud, K.Y., 2023. Trends in paper-based sensing devices for clinical and environmental monitoring. Biosensors 13. https://doi.org/10.3390/bios13040420.

Laboratory testing for 2019 novel coronavirus (2019-nCoV) in suspected human cases [WWW Document], n.d. URL https://www.who.int/publications/i/item/10665-331501 (accessed 3.July.2023).

Lacroix, A., Sleiman, H.F., 2021. DNA nanostructures: current challenges and opportunities for cellular delivery. ACS Nano 15, 3631–3645. https://doi.org/10.1021/acsnano.0c06136.

Lazaro, A., Villarino, R., Lazaro, M., Canellas, N., Prieto-Simon, B., Girbau, D., 2022. Battery-less NFC potentiostat for electrochemical point-of-care sensors based on COTS components. Sensors 22. https://doi.org/10.3390/s22197213.

Lisboa Bastos, M., Tavaziva, G., Abidi, S.K., Campbell, J.R., Haraoui, L.P., Johnston, J.C., Lan, Z., Law, S., MacLean, E., Trajman, A., Menzies, D., Benedetti, A., Khan, F.A., 2020. Diagnostic accuracy of serological tests for covid-19: systematic review and meta-analysis. BMJ 370. https://doi.org/10.1136/BMJ.M2516.

Lisi, F., Peterson, J.R., Gooding, J.J., 2020. The application of personal glucose meters as universal point-of-care diagnostic tools. Biosens. Bioelectron. 148 https://doi.org/10.1016/j.bios.2019.111835.

Lukas, H., Xu, C., Yu, Y., Gao, W., 2020. Emerging telemedicine tools for remote covid-19 diagnosis, monitoring, and management. ACS Nano 14, 16180–16193. https://doi.org/10.1021/ACSNANO.0C08494/ASSET/IMAGES/MEDIUM/NN0C08494_0006.GIF.

Ma, L., Cheng, C., Liu, X., Zhao, Y., Wang, A., Herdewijn, P., 2004. A neural network for predicting the stability of RNA/DNA hybrid duplexes. Chemometr. Intell. Lab. Syst. 70, 123–128. https://doi.org/10.1016/j.chemolab.2003.10.002.

Maroli, G., Aymonino, O.A., Oliva, A., Gak, J., Julian, P., Palumbo, F., 2023. Printed electronics: a low-cost alternative to prototyping in the academic field. In: 2023 Argentine Conf. Electron, pp. 69–74. https://doi.org/10.1109/CAE56623.2023.10086979. CAE 2023 - Congr. Argentino Electron. 2023, CAE 2023.

Martynenko, I.V., Ruider, V., Dass, M., Liedl, T., Nickels, P.C., 2021. DNA origami meets bottom-up nanopatterning. ACS Nano 15, 10769–10774. https://doi.org/10.1021/acsnano.1c04297.

Matharu, Z., Daggumati, P., Wang, L., Dorofeeva, T.S., Li, Z., Seker, E., 2017. Nanoporous-gold-based electrode morphology libraries for investigating structure-property relationships in nucleic acid based electrochemical biosensors. ACS Appl. Mater. Interfaces 9, 12959–12966. https://doi.org/10.1021/acsami.6b15212.

McCoy, C.A., 2023. How does the pandemic end? Losing control of the COVID-19 pandemic illness narrative. Global Publ. Health 18. https://doi.org/10.1080/17441692.2023.2195918.

Moya, A., Gabriel, G., Villa, R., Javier del Campo, F., 2017. Inkjet-printed electrochemical sensors. Curr. Opin. Electrochem. 3, 29–39. https://doi.org/10.1016/j.coelec.2017.05.003.

Msemburi, W., Karlinsky, A., Knutson, V., Aleshin-Guendel, S., Chatterji, S., Wakefield, J., 2023. The WHO estimates of excess mortality associated with the COVID-19 pandemic. Nature 613, 130–137. https://doi.org/10.1038/s41586-022-05522-2.

Murray, C.J.L., 2022. COVID-19 will continue but the end of the pandemic is near. Lancet 399, 417–419. https://doi.org/10.1016/S0140-6736(22)00100-3.

Nicholson, R.S., 1965. Theory and application of cyclic voltammetry for measurement of electrode reaction kinetics. Anal. Chem. 37, 1351–1355. https://doi.org/10.1021/AC60230A016/ASSET/AC60230A016. FP.PNG_V03.

Nicholson, R.S., Shain, I., 1964. Theory of stationary electrode polarography: single scan and cyclic methods applied to reversible, irreversible, and kinetic systems. Anal. Chem. 36, 706–723. https://doi.org/10.1021/AC60210A007/ASSET/AC60210A007.FP.PNG_V03.

Owczarzy, R., Vallone, P.M., Gallo, F.J., Paner, T.M., Lane, M.J., Benight, A.S., 1997. Predicting sequence-dependent melting stability of short duplex DNA oligomers. Biopolymers 44, 217–239. https://doi.org/10.1002/(sici)1097-0282 (1997)44:3<217::aid-bip3>3.0.co;2-y.

Pan, S., Rothberg, L., 2005. Chemical control of electrode functionalization for detection of DNA hybridization by electrochemical impedance spectroscopy. Langmuir 21, 1022–1027. https://doi.org/10.1021/la048083a.

Panicker, L.R., Kummari, S., Keerthanaa, M.R., Rao Bommi, J., Koteshwara Reddy, K., Yugender Goud, K., 2024. Trends and challenges in electroanalytical biosensing methodologies for infectious viral diseases. Bioelectrochemistry 156, 108594. https://doi.org/10.1016/J.BIOELECHEM.2023.108594.

Park, S., Kim, H.C., Chung, T.D., 2012. Electrochemical analysis based on nanoporous structures. Analyst 137, 3891–3903. https://doi.org/10.1039/c2an35294j.

Peeling, R.W., Heymann, D.L., Teo, Y.Y., Garcia, P.J., 2022. Diagnostics for COVID-19: moving from pandemic response to control. Lancet (London, England) 399, 757. https://doi.org/10.1016/S0140-6736(21)02346-1.

Pheeney, C.G., Barton, J.K., 2012. DNA electrochemistry with tethered methylene blue. Langmuir 28, 7063–7070. https://doi.org/10.1021/la300566x.

Piro, B., Haccoun, J., Pham, M.C., Tran, L.D., rubin, A., Perrot, H., Gabrielli, C., 2005. Study of the DNA hybridization transduction behavior of a quinone-containing electroactive polymer by cyclic voltammetry and electrochemical impedance spectroscopy. J. Electroanal. Chem. 577, 155–165. https://doi.org/10.1016/j.jelechem.2004.12.002.

Poli, E., Jong, K.H., Hassanali, A., 2020. Charge transfer as a ubiquitous mechanism in determining the negative charge at hydrophobic interfaces. Nat. Commun. 111 (11), 1–13. https://doi.org/10.1038/s41467-020-14659-5, 2020.

Post, N., Eddy, D., Huntley, C., van Schalkwyk, M.C.I., Shrotri, M., Leeman, D., Rigby, S., Williams, S.V., Bermingham, W.H., Kellam, P., Maher, J., Shields, A.M., Amirthalingam, G., Peacock, S.J., Ismail, S.A., 2020. Antibody response to SARS-CoV-2 infection in humans: a systematic review. PLoS One 15, e0244126. https://doi.org/10.1371/JOURNAL.PONE.0244126.

Promsuwan, K., Soleh, A., Samoson, K., Saisahas, K., Wangchuk, S., Saichanapan, J., Kanatharana, P., Thavarungkul, P., Limbut, W., 2023. Novel biosensor platform for glucose monitoring via smartphone based on battery-less NFC potentiostat. Talanta 256. https://doi.org/10.1016/j.talanta.2023.124266.

Pungjunun, K., Yakoh, A., Chaiyo, S., Siangproh, W., Praphairaksit, N., Chailapakul, O., 2022. Smartphone-based electrochemical analysis integrated with NFC system for the voltammetric detection of heavy metals using a screen-printed graphene electrode. Microchim. Acta 189. https://doi.org/10.1007/s00604-022-05281-x.

Qiu, G., Gai, Z., Tao, Y., Schmitt, J., Kullak-Ublick, G.A., Wang, J., 2020. Dual-functional plasmonic photothermal biosensors for highly accurate severe acute respiratory syndrome coronavirus 2 detection. ACS Nano 14, 5268–5277. https://doi.org/10.1021/ACSNANO.0C02439/SUPPL_FILE/NN0C02439_SI_001.PDF.

Ranallo, S., Bracaglia, S., Sorrentino, D., Ricci, F., 2023. Synthetic antigen-conjugated DNA systems for antibody detection and characterization. ACS Sens. 8, 2415–2426. https://doi.org/10.1021/acssensors.3c00564.

Rao Bommi, J., Kummari, S., Lakavath, K., Sukumaran, R.A., Panicker, L.R., Marty, J.L., Yugender Goud, K., 2023. Recent trends in biosensing and diagnostic methods for novel cancer biomarkers. Biosensors 13. https://doi.org/10.3390/BIOS13030398.

Ricci, F., Dietz, H., 2023. The harmony of form and function in DNA nanotechnology. Nat. Nanotechnol. https://doi.org/10.1038/s41565-023-01362-x.

Rosati, G., Idili, A., Parolo, C., Fuentes-Chust, C., Calucho, E., Hu, L., Castro E Silva, C.D. C., Rivas, L., Nguyen, E.P., Bergua, J.F., Alvárez-Diduk, R., Muñoz, J., Junot, C., Penon, O., Monferrer, D., Delamarche, E., Merkoçi, A., 2021. Nanodiagnostics to face SARS-CoV-2 and future pandemics: from an idea to the market and beyond. ACS Nano 15, 17137–17149. https://doi.org/10.1021/ACSNANO.1C06839.

Rosati, G., Urban, M., Zhao, L., Yang, Q., de Carvalho Castro e Silva, C., Bonaldo, S., Parolo, C., Nguyen, E.P., Ortega, G., Fornasiero, P., Paccagnella, A., Merkoçi, A., 2022. A plug, print & play inkjet printing and impedance-based biosensing technology operating through a smartphone for clinical diagnostics. Biosens. Bioelectron. 196 https://doi.org/10.1016/j.bios.2021.113737.

Rossetti, M., Brannetti, S., Mocenigo, M., Marini, B., Ippodrino, R., Porchetta, A., 2020. Harnessing effective molarity to design an electrochemical DNA-based platform for clinically relevant antibody detection. Angew. Chem. Int. Ed. 59, 14973–14978. https://doi.org/10.1002/anie.202005124.

Rossetti, M., Porchetta, A., 2018. Allosterically regulated DNA-based switches: from design to bioanalytical applications. Anal. Chim. Acta 1012, 30–41. https://doi.org/10.1016/j.aca.2017.12.046.

Rowe, A.A., Chuh, K.N., Lubin, A.A., Miller, E.A., Cook, B., Hollis, D., Plaxco, K.W., 2011. Electrochemical biosensors employing an internal electrode attachment site and achieving reversible, high gain detection of specific nucleic acid sequences. Anal. Chem. 83, 9462–9466. https://doi.org/10.1021/ac202171x.

Rubio-Monterde, A., Quesada-González, D., Merkoçi, A., 2023. Toward integrated molecular lateral flow diagnostic tests using advanced micro- and nanotechnology. Anal. Chem. 95, 468–489. https://doi.org/10.1021/ACS.ANALCHEM.2C04529/ASSET/IMAGES/ACS.ANALCHEM.2C04529.SOCIAL. JPEG_V03.

Santhanam, M., Algov, I., Alfonta, L., 2020. DNA/RNA electrochemical biosensing devices a future replacement of PCR methods for a fast epidemic containment. Sensors 20, 1–15. https://doi.org/10.3390/s20164648.

Sarker, R., Roknuzzaman, A.S.M., Nazmunnahar, Shahriar, M., Hossain, M.J., Islam, M. R., 2023. The WHO has declared the end of pandemic phase of COVID-19: way to come back in the normal life. Heal. Sci. Reports 6. https://doi.org/10.1002/hsr2.1544.

Sathish, V., Manivannan, C., Balasubramaniyan, M., Kumar, A.R., Thanasekaran, P., 2021. Advances of inorganic materials in the detection and therapeutic uses against coronaviruses. Curr. Med. Chem. 28, 5311–5327. https://doi.org/10.2174/0929867328666210219142208.

Schöley, J., Karlinsky, A., Kobak, D., Tallack, C., 2023. Conflicting COVID-19 excess mortality estimates. Lancet 401, 431–432. https://doi.org/10.1016/S0140-6736(23)00116-2.

Steinberg, M.D., Kassal, P., Kereković, I., Steinberg, I.M., 2015. A wireless potentiostat for mobile chemical sensing and biosensing. Talanta 143, 178–183. https://doi.org/10.1016/j.talanta.2015.05.028.

Su, Z., Kim, C.O., Renner, J.N., 2021. Quantification of the effects of hydrophobicity and mass loading on the effective coverage of surface-immobilized elastin-like peptides. Biochem. Eng. J. 168, 107933 https://doi.org/10.1016/J.BEJ.2021.107933.

Sugimoto, N., Katoh, M., Nakano, S. -i., Ohmichi, T., Sasaki, M., 1994. RNA/DNA hybrid duplexes with identical nearest-neighbor base-pairs have identical stability. FEBS Lett. 354, 74–78. https://doi.org/10.1016/0014-5793(94)01098-6.

Sugimoto, N., Nakano, S.-I., Katoh, M., Matsumura, A., Nakamuta, H., Ohmichi, T., Yoneyama, M., Sasaki, M., 1995. Thermodynamic parameters to predict stability of RNA/DNA hybrid duplexes. Biochemistry 34, 11211–11216. https://doi.org/10.1021/bi00035a029.

Sundriyal, P., Bhattacharya, S., 2017. Inkjet-printed electrodes on A4 paper substrates for low-cost, disposable, and flexible asymmetric supercapacitors. ACS Appl. Mater. Interfaces 9, 38507–38521. https://doi.org/10.1021/acsami.7b11262.

Tagliaferri, S., Nagaraju, G., Panagiotopoulos, A., Och, M., Cheng, G., Iacoviello, F., Mattevi, C., 2021. Aqueous inks of pristine graphene for 3D printed microsupercapacitors with high capacitance. ACS Nano 15, 15342–15353. https://doi.org/10.1021/acsnano.1c06535.

Tombuloglu, H., Sabit, H., Al-Khallaf, H., Kabanja, J.H., Alsaeed, M., Al-Saleh, N., Al-Suhaimi, E., 2022. Multiplex real-time RT-PCR method for the diagnosis of SARS-CoV-2 by targeting viral N, RdRP and human RP genes. Sci. Rep. 12 https://doi.org/10.1038/s41598-022-06977-z.

Udugama, B., Kadhiresan, P., Kozlowski, H.N., Malekjahani, A., Osborne, M., Li, V.Y.C., Chen, H., Mubareka, S., Gubbay, J.B., Chan, W.C.W., 2020a. Diagnosing COVID-19: the disease and tools for detection. ACS Nano 14, 3822–3835. https://doi.org/10.1021/ACSNANO.0C02624/ASSET/IMAGES/LARGE/NN0C02624_0004. JPEG.

Udugama, B., Kadhiresan, P., Kozlowski, H.N., Malekjahani, A., Osborne, M., Li, V.Y.C., Chen, H., Mubareka, S., Gubbay, J.B., Chan, W.C.W., 2020b. Diagnosing COVID-19: the disease and tools for detection. ACS Nano 14, 3822–3835. https://doi.org/10.1021/ACSNANO.0C02624/ASSET/IMAGES/LARGE/NN0C02624_0004. JPEG.

Urban, M., Rosati, G., Maroli, G., Pelle, F. Della, Bonini, A., Sajti, L., Fedel, M., Merkoçi, A., 2023. Nanostructure tuning of gold nanoparticles films via click sintering. Small 2306167. https://doi.org/10.1002/smll.202306167.

Wang, B., Wang, L., Kong, X., Geng, J., Xiao, D., Ma, C., Jiang, X.-M., Wang, P.-H., 2020. Long-term coexistence of SARS-CoV-2 with antibody response in COVID-19 patients. J. Med. Virol. 92, 1684–1689. https://doi.org/10.1002/jmv.25946.

Wang, H., Paulson, K.R., Pease, S.A., Watson, S., Comfort, H., Zheng, P., Aravkin, A.Y., Bisignano, C., Barber, R.M., Alam, T., Gakidou, E., Murray, C.J.L., 2022. Estimating excess mortality due to the COVID-19 pandemic: a systematic analysis of COVID-19-related mortality, 2020–21. Lancet 399, 1513–1536. https://doi.org/10.1016/S0140-6736(21)02796-3.

Wang, Q., Iketani, S., Li, Z., Liu, L., Guo, Y., Huang, Y., Bowen, A.D., Liu, M., Wang, M., Yu, J., Liu, L., Ho, D.D., 2023. Alarming antibody evasion properties of rising SARS-CoV-2 BQ and XBB subvariants. Cell 186, 279–286. https://doi.org/10.1016/j.cell.2022.12.018.

Wei, F., Sun, B., Guo, Y., Zhao, X.S., 2003. Monitoring DNA hybridization on alkyl modified silicon surface through capacitance measurement. Biosens. Bioelectron. 18, 1157–1163. https://doi.org/10.1016/S0956-5663(03)00002-2.

Weiss, C., Carriere, M., Fusco, L., Fusco, L., Capua, I., Regla-Nava, J.A., Pasquali, M., Pasquali, M., Pasquali, M., Scott, J.A., Vitale, F., Vitale, F., Unal, M.A., Mattevi, C., Bedognetti, D., Merkoçi, A., Merkoçi, A., Tasciotti, E., Tasciotti, E., Yilmazer, A., Yilmazer, A., Gogotsi, Y., Stellacci, F., Delogu, L.G., 2020. Toward nanotechnology-enabled approaches against the COVID-19 pandemic. ACS Nano 14, 6383–6406. https://doi.org/10.1021/ACSNANO.0C03697.

Wise, J., 2023. Covid-19: WHO declares end of global health emergency. BMJ 381, p1041. https://doi.org/10.1136/bmj.p1041.

Xiao, Y., Lai, R.Y., Plaxco, K.W., 2007. Preparation of electrode-immobilized, redox-modified oligonucleotides for electrochemical DNA and aptamer-based sensing. Nat. Protoc. 2, 2875–2880. https://doi.org/10.1038/nprot.2007.413.

Zhang, R., Chen, R., Ma, Y., Liang, J., Ren, S., Gao, Z., 2023. Application of DNA Nanotweezers in biosensing: nanoarchitectonics and advanced challenges. Biosens. Bioelectron. 237 https://doi.org/10.1016/j.bios.2023.115445.

G. Maroli, A. Fontana, S. M. Pazos, F. Palumbo and P. Julián, "A Geometric Modeling Approach for Flexible, Printed Square Planar Inductors under Stretch," 2021 Argentine Conference on Electronics (CAE), Bahia Blanca, Argentina, 2021, pp. 61-66, doi: 10.1109/CAE51562.2021.9397568.